pected that, when the unknown $d_{yz} \rightarrow d_{z^2}$ promotion energy barrier is exceeded by an appropriate interaction with external sources of energy, even the square-planar complex could react with dioxygen.

Acknowledgment. We wish to thank the Accademia Nazionale dei Lincei for computing facilities and travel expenses. We wish to thank Professor R. Ugo for helpful discussions.

References and Notes

(1) B. M. Hoffman, D. L. Diemente, and F. Basolo, *J. Am. Chem. Soc.*, **92,** 61 (1970).
(2) B. M. Hoffman and D. H. Petering, *Proc. Natl. Acad. Sci.*, **67,** 637 (1970).
(3) F. A. Walker, *J. Am. Chem. Soc.*, **92**, 4235 (1970); D. V. Stynes, H. C. Stynes, B. R. James, and J. A. Ibers, *ibid.*, **95**, 1796 (1973).
(4) E.-J. Ochiai, *Inorg. Nucl. Chem.*, **35**, 3375 (1973).
(5) D. M. Mingos, *Nature* (*London*) *Phys. Sci.*, **230,** 154 (1971).
(6) C. Busetto, F. Cariati, A. Fusi, M. Gullotti, F. Morazzoni, A. Pasini, R. Ugo, and V. Valenti, *J. Chem. Soc., Dalton Trans.*, 754 (1973).
(7) L. M. Engelhardt and M. Green, *J. Chem. Soc., Dalton Trans.*, 724 (1972), and references cited therein.
(8) C. J. Ballhausen and H. B. Gray, "Molecular Orbital Theory", W. A. Benjamin, New York, N.Y., 1975.
(9) J. A. Pople and D. L. Beveridge, "Approximate Molecular Orbital Theory", Mc-Graw Hill, New York, N.Y., 1970.
(10) J. A. Pople and R. K. Nesbet, *J. Chem. Phys.*, **22,** 571 (1954).
(11) K. Nishimoto and M. Mataga, *Z. Phys. Chem.*, **12,** 335 (1957); **13,** 140 (1957).
(12) D. W. Clack, N. S. Hush, and J. R. Yandle, *J. Chem. Phys.*, **57**, 3504 (1972).
(13) L. Oleari, L. Di Sipio and G. De Michelis, *Mol. Phys.*, **10,** 97 (1966); L. Di Sipio, E. Tondello, G. De Michelis, and L. Oleari, *Chem. Phys. Lett.*, **11,** 287 (1971).
(14) J. Hinze and H. H. Jaffé, *J. Chem. Phys.*, **38,** 1843 (1963).
(15) A. T. Amos and G. G. Hall, *Proc. R. Soc. London, Ser. A*, **263,** 483 (1961)
(16) R. McWeeney, *Proc. R. Soc. London, Ser. A*, **235,** 496 (1956).
(17) E. Clementi and L. Raimondi, *J. Chem. Phys.*, **38,** 2686 (1963).
(18) M. Gouterman and Z. Zerner, *Theor. Chim. Acta*, **4,** 44 (1966).
(19) S. Brükner, M. Calligaris, G. Nardin, and L. Randaccio, *Inorg. Chim. Acta*, **2,** 386 (1968).
(20) P. Fantucci, V. Valenti, F. Cariati, and I. Fragalà, *Inorg. Nucl. Chem. Lett.*, **11,** 585 (1975).
(21) G. Condorelli, I. Fragalà, A. Centineo, and E. Tondello, *Inorg. Chim. Acta*, **7,** 725 (1973).
(22) G. De Alti, V. Galasso, and A. Bigotto, *Inorg. Chim. Acta*, **6,** 129 (1972).
(23) B. M. Hoffman, F. Basolo, and D. L. Diemente, *J. Am. Chem. Soc.*, **95,** 6497 (1973).
(24) A. von Zelewsky and H. Fierz, *Helv. Chim. Acta*, **56,** 3 (1973).
(25) F. Cariati, F. Morazzoni, C. Busetto, D. Del Piero, and A. Zazzetta, *J. Chem. Soc., Dalton Trans.*, 342 (1976).
(26) (a) N. S. Hush and I. S. Woolsey, *J. Chem. Soc., Dalton Trans.*, 24 (1974); (b) A. H. Maki, N. Edelstein, A. Davidson, and R. H. Holm, *J. Am. Chem. Soc.*, **66,** 4580 (1964).
(27) C. Floriani and F. Calderazzo, *J. Chem. Soc. A*, 946 (1969).
(28) M. J. Carter, D. P. Rillema, and F. Basolo, *J. Am. Chem. Soc.*, **96,** 392 (1974).
(29) M. Calligaris, D. Minichelli, G. Nardin, and L. Randaccio, *J. Chem. Soc. A*, 2412 (1970).
(30) B. A. Goodman and J. B. Raynor, *Adv. Inorg. Chem. Radiochem.*, **13,** 1 (1970).
(31) J. S. Griffith, "The Theory of Transition-Metal Ions", Cambridge University Press, London, 1961, p 373.
(32) R. McWeeney, "Spins in Chemistry", Academic Press, New York, N.Y., 1970.
(33) M. Calligaris, G. Nardin, L. Randaccio, and G. Tauzher, *Inorg. Nucl. Chem. Lett.*, **9,** 419 (1973).
(34) G. A. Rodley and W. T. Robinson, *Nature* (*London*), **235,** 438 (1972).
(35) C. Busetto, F. Cariati, P. Fantucci, D. Galizzioli, F. Morazzoni, and V. Valenti, *Gazz. Chim. Ital.*, **102,** 1040 (1972).
(36) A. Dedieu and A. Veillard, *Theor. Chim. Acta*, **36,** 231 (1975).
(37) A. E. Martell and M. Calvin, "Chemistry of Metal Chelate Compounds", Prentice-Hall, Engelwood Cliff, N.J., 1959.
(38) L. G. Marzilli, P. A. Marzilli, and J. Halpern, *J. Am. Chem. Soc.*, **93,** 1374 (1971).
(39) (a) M. Tamaki, I. Masuda, and K. Shimra, *Bull. Chem. Soc. Jpn.*, **42,** 2858 (1969); (b) A. Earnshaw, P. C. Hewlett, and F. Larkwortthy, *J. Chem. Soc. A*, 4718 (1965); (c) E. Lester, *Inorg. Chem.*, **12, 244** (1973).
(40) B. B. Wayland and D. Mohaier, *J. Am. Chem. Soc.*, **93**, 5295 (1971).
(41) F. Cariati, D. Galizzioli, F. Morazzoni, and C. Busetto, *J. Chem. Soc., Dalton Trans.*, 556 (1975).
(42) F. A. Walker, *J. Am. Chem. Soc.*, **95,** 1150 (1973).
(43) G. Henrici-Olivé and S. Olivé, *Angew. Chem. Int. Ed. Engl.*, **13**, 29 (1974).
(44) S. C. Abraham, *Q. Rev. Chem. Soc.*, **10,** 407 (1956).
(45) Y. B. Taarit and J. H. Lunsford, *J. Phys. Chem.*, **77,** 870 (1973), and references cited therein.
(46) R. J. Celotta, R. A. Bennett, J. R. Hall, M. W. Siegel, and J. Levine, *Phys. Rev.* (*Sect.*) *A*, **6,** 631 (1972).
(47) M. Krauss, D. Neumann, A. C. Wahl, G. Das, and W. Zemke, *Phys. Rev. Sect. A*, **7,** 69 (1973); W. T. Zemke, G. Das, and A. C. Wahl, *Chem. Phys. Lett.*, **14,** 310 (1972).
(48) B. S. Tovrog and R. S. Drago, *J. Am. Chem. Soc.*, **96,** 6765 (1974), and private communication.
(49) B. M. Hoffman, T. Szymanki, and F. Basolo, *J. Am. Chem. Soc.*, **97,** 673 (1975).
(50) D. V. Stynes, H. C. Stynes, J. A. Ibers, and B. R. James, *J. Am. Chem. Soc.*, **95,** 1142 (1973).
(51) M. Calligaris, G. Nardin, L. Randaccio, and A. Ripamonti, *J. Chem. Soc. A*, 1069 (1970).

Localized Molecular Orbital Studies of Chemical Reactions. Deformation, Rearrangement, and Spin Polarization of Bonds Involved in Radical Reactions

Shigeru Nagase, Kazuo Takatsuka, and Takayuki Fueno*

Contribution from the Department of Chemistry, Faculty of Engineering Science, Osaka University, Toyonaka, Osaka, Japan. *Received March 11, 1975*

Abstract: Energy-localized molecular orbitals (LMO) generated from UHF-INDO wave functions have been used for the studies of the mechanism of abstraction and addition reactions of doublet radicals. The UHF wave functions for reacting systems have been interpreted in terms of the LMO mapping and the intermolecular configuration interaction. The deformation, rearrangement, and spin polarization of bonds developing with the progress of reaction can most conveniently be visualized in these terms. The whole aspects of the reactions are pictorially demonstrated by tracing the movements of the LMO charge centroids. It is concluded that both reactions appear to proceed by a three-stage mechanism which involves the successive β- and α-spin electron transfers and the concomitant spin polarization associated with particular LMO's. A possible relationship of the proposed mechanism with orbital crossing is discussed.

The formation of chemical bonds has recently been analyzed by several authors[1-3] from a rigorous quantum-mechanical viewpoint. Practically, however, rigorous treatments are not only too tedious to be manageable in general cases, but are often liable to complicate a simple and vivid picture of chemical reactions commonly used by the chemist. Thus, it seems of practical value to seek convenient procedures which could give us chemically meaningful visualization and interpretation of chemical reactions, with the concept of an electron pair bond preserved. Efforts along this line would indeed be rewarding if they could serve to establish a bridge between the conventional ideas of chemical reactions and the wave-mechanical pictures of chemical interactions.

We think that one of the most appealing procedures is the use of localized molecular orbitals (LMO). Perhaps the most successful and widely used procedure for obtaining LMO's has been the one which was put forth by Lennard-Jones and Pople[4] and developed by Edmiston and Ruedenberg.[5] The theory has already been applied to a number of molecules in the closed-shell ground singlet state, and the results in most cases are in harmony with the conventional pictures of chemical bonding. Applications to interacting systems such as the protonated complexes of aldehyde,[6] methane,[7] and ethylene[8] have been reported recently. However, there have been few calculations available so far for open-shell molecules,[9-11] still less for their chemical interactions.

In this paper, we deal with the abstraction and addition reactions of doublet radicals in terms of the unrestricted Hartree-Fock (UHF) LMO's. Our specific aim is to elucidate mechanistic details of the bond rearrangement involved in radical reactions. To this end, we will map the UHF LMO's of an entire reacting system at given path points over those for isolated molecules in order to analyze the course of bond deformations. Also, the UHF wave functions of the reacting system will be expanded as a superposition of various electronic configurations of reactant molecules. Prototype reactions worked out along these lines show that both abstraction and addition reactions of radicals appear to proceed by a three-stage mechanism which involves successive β- and α-spin electron transfer followed by spin polarization of the reacting bond.

I. General Consideration

A. Three-Electron Model. Localized molecular orbital studies of chemical reactions have one unique merit in that the behavior of electrons during reaction can be visualized in close relation to the deformation of the bonds and nonbonding orbitals present. Thus, a substantial part of the reaction mechanism can be reduced to the local behavior of particular LMO's directly associated with the reaction site. Under this notion, we will here outline a characteristic feature of radical reactions in a simple but general manner.

In the LMO treatment of the abstraction and addition reactions of doublet radicals, it may suffice to consider only the two electrons in the reaction bond of the substrate and one α-spin electron from the radical. Denote the occupied and vacant LMO's of the bond by a and a^*, respectively, and the LMO of the radical by b. These LMO's will suffer deformation as the substrate and radical interact with each other. The occupied LMO's thus deformed may be expressed as

$$\psi_a = k_1 a + k_2 a^* + k_3 b \tag{1}$$

$$\bar{\psi}_a = k_4 \bar{a} + k_5 \bar{a}^* + k_6 \bar{b} \tag{2}$$

$$\psi_b = k_7 b + k_8 a^* + k_9 a \tag{3}$$

where a bar over LMO stands for the β-spin.

Using eq 1-3, we can expand the UHF single-determinantal wave function of the interacting system Ψ_{UHF} as a superposition of various electronic configurations of reactant molecules:

$$\Psi_{\mathrm{UHF}} = |\psi_a \bar{\psi}_a \psi_b| = \sum_K C_K \Phi_K \tag{4}$$

where Φ_K's are the configurations specified as follows:

$$\Phi_{\mathrm{G}} = |a\bar{a}b| \tag{5}$$

$$\Phi_{\mathrm{CT}} = |a\bar{b}b| \tag{6}$$

$$\Phi_{\mathrm{BCT}} = |a\bar{a}a^*| \tag{7}$$

$$\Phi_{\mathrm{LE}}{}^{\mathrm{S}} = (\sqrt{2})^{-1}[|a\bar{a}^*b| - |\bar{a}a^*b|] \tag{8}$$

$$\Phi_{\mathrm{LE}}{}^{\mathrm{T}} = (\sqrt{6})^{-1}[|a\bar{a}^*b| + |\bar{a}a^*b| - 2|aa^*\bar{b}|] \tag{9}$$

$$\Phi_{\mathrm{LE}}{}^{\mathrm{Q}} = (\sqrt{3})^{-1}[|a\bar{a}^*b| + |\bar{a}a^*b| + |aa^*\bar{b}|] \tag{10}$$

$$\Phi_{\mathrm{CT\cdot LE}} = |a^*\bar{b}b| \tag{11}$$

$$\Phi_{\mathrm{BCT\cdot LE}} = |a\bar{a}^*a^*| \tag{12}$$

and

$$\Phi_{\mathrm{LDE}} = |a^*\bar{a}^*b| \tag{13}$$

Here, Φ_{G} is the lowest energy configuration; Φ_{CT}, the configuration arising from the β-spin electron transfer from substrate to radical; Φ_{BCT}, the back α-spin electron transfer from radical to substrate; $\Phi_{\mathrm{LE}}{}^{\mathrm{S}}$, the local singlet excitation of the substrate; $\Phi_{\mathrm{LE}}{}^{\mathrm{T}}$, the local triplet excitation of the substrate; $\Phi_{\mathrm{LE}}{}^{\mathrm{Q}}$ is the quartet component which is inevitably involved in Ψ_{UHF} as an undesirable contamination; $\Phi_{\mathrm{CT\cdot LE}}$, the β-spin electron transfer from substrate to radical followed by the local excitation of the substrate; $\Phi_{\mathrm{BCT\cdot LE}}$, the back α-spin electron transfer from radical to substrate followed by the local excitation of the substrate; and Φ_{LDE}, the local double excitation of the substrate. The configurational coefficients C_K are dependent on the various coefficients k_{m} appearing in eq 1-3.

Let us assume for a moment that $k_1 = k_4 = k_7 = 1$ and $k_3 = k_9 = 0$. The assumption is in fact permissible at an early stage of reaction, as will be shown later. Neglecting the terms second order in the remaining coefficients k_m, one can rewrite eq 4 into

$$\Psi_{\mathrm{UHF}} \simeq \Phi_{\mathrm{G}} + k_6\Phi_{\mathrm{CT}} + k_8\Phi_{\mathrm{BCT}} + (\sqrt{2})^{-1}(k_2 + k_5)\Phi_{\mathrm{LE}}{}^{\mathrm{S}} + (\sqrt{6})^{-1}(k_5 - k_2)\Phi_{\mathrm{LE}}{}^{\mathrm{T}} + (\sqrt{3})^{-1}(k_5 - k_2)\Phi_{\mathrm{LE}}{}^{\mathrm{Q}} \tag{14}$$

In eq 14, $(k_2 + k_5)$ must be small in magnitude as compared with $(k_5 - k_2)$, because k_2 and k_5 should take on values in different signs. Thus, the mixing of the antibonding LMO a^* into bonding LMO a with different signs for the α- and β-spin electrons is tantamount to the inducement of triplet excitation $\Phi_{\mathrm{LE}}{}^{\mathrm{T}}$ in the substrate bond. However, the mixing involves the quartet excitation $\Phi_{\mathrm{LE}}{}^{\mathrm{Q}}$ also. The coefficients k_6 and k_8 are, as they should be, related with the β-spin electron transfer from substrate to radical Φ_{CT} and the back α-spin electron transfer from radical to substrate Φ_{BCT}, respectively.

It is apparent from the foregoing considerations that the evaluation of the coefficients k_m's in eq 1-3 is of fundamental value for the understanding of the variation in electronic structure of a chemical bond undergoing radical reaction. The deformation, rearrangement, and spin polarization of a reacting bond can be disclosed most conveniently by this method. It is for this merit that we here propose the use of LMO mappings for the studies of reactions of open-shell molecules.

B. General Cases. In more precise treatments we take account of all the LMO's involved. As a chemical reaction proceeds, the LMO's of two interacting molecules are more or less delocalized from one molecule to the other. Some of the initial LMO's are thus deformed progressively, until they are collapsed and other newly definable LMO's begin to take over. The process is no doubt closely related to the rearrangement of chemical bonds during reaction.

Consider two molecules R and S with the LMO's $\psi_{\mathrm{R}}{}^{\gamma}$ and $\psi_{\mathrm{S}}{}^{\gamma}$, respectively, where the superscript γ denotes the α- or β-spin. Each spin set of LMO's, involving both the occupied and vacant orbitals, are usually expressed as a linear combination of atomic orbitals $\mathbf{X}_{\mathrm{R}}$ or $\mathbf{X}_{\mathrm{S}}$. In the absence of interaction, the LMO's $\psi_0{}^{\gamma}$ of the entire system are written as

$$\psi_0{}^{\gamma} = \mathbf{X}\mathbf{C}_0{}^{\gamma} \tag{15}$$

with the row vectors

$$\psi_0{}^\gamma = (\psi_R{}^\gamma\ \psi_S{}^\gamma),\ \mathbf{X} = (\mathbf{X}_R\ \mathbf{X}_S) \tag{16}$$

and a square matrix

$$\mathbf{C}_0{}^\gamma = \begin{pmatrix} \mathbf{C}_R{}^\gamma & 0 \\ 0 & \mathbf{C}_S{}^\gamma \end{pmatrix} \tag{17}$$

where $\mathbf{C}_R{}^\gamma$ and $\mathbf{C}_S{}^\gamma$ are the LCAO matrices for $\psi_R{}^\gamma$ and $\psi_S{}^\gamma$, respectively. The LMO's ψ^γ deformed by the perturbation in the interacting system can also be represented by use of a similar notation

$$\psi^\gamma = \mathbf{X}\mathbf{C}^\gamma \tag{18}$$

The matrix $\mathbf{C}^\gamma$ can no longer be expressed in such a block form as eq 17.

We now define a matrix $\mathbf{T}^\gamma$ such that

$$\mathbf{T}^\gamma = (\mathbf{C}_0{}^\gamma)^{-1}\mathbf{C}^\gamma \tag{19}$$

If the AO's $\mathbf{X}_R$ and $\mathbf{X}_S$ are orthogonal and normalized in such a way as in the INDO approximation, $\mathbf{C}^\gamma$, as well as $\mathbf{C}_0{}^\gamma$, is a unitary matrix and so is $\mathbf{T}^\gamma$. From eq 15, 18, and 19, it follows that

$$\psi^\gamma = \psi_0{}^\gamma\mathbf{T}^\gamma \tag{20}$$

which, in an algebraic form, is

$$\psi_i{}^\gamma = \sum_m^R t_{mi}{}^\gamma\psi_{Rm}{}^\gamma + \sum_n^S t_{ni}{}^\gamma\psi_{Sn}{}^\gamma \tag{21}$$

where the first sum is over the LMO's of molecule R while the second over those of molecule S. The LMO's for the interacting system is thus mapped over those for the isolated molecules R and S.

A chemical reaction generally involves the displacement of nuclei in the reactant molecules, which should alter the phase (or nodal) structures of the LMO's. For example, bendings and stretchings at a certain center would alter the hybridization of the basis functions on that center, and a twist would alter the orientation of the p-type basis functions on the affected center. In order to cope with the situation, we adopt Trindle's mapping method[12] and make the LMO's of reactant molecules match those of interacting molecules as much as possible in a topological sense. That is, we employ as $\psi_0{}^\gamma$ those LMO's constrained to a topological identity.

A set of UHF LMO's obtained at a given path point may then be used to construct the UHF ground-state wave function Ψ_{UHF} at that point. The function can be expanded into various electronic configurations:

$$\begin{aligned}\Psi_{UHF} &= |\psi_1{}^\alpha\psi_1{}^\beta \ldots \psi_p{}^\alpha\psi_p{}^\beta\psi_{p+1}{}^\alpha| \\ &= C_G\Phi_G + \sum_K\sum_j C_{Kj}\Phi_{Kj}\end{aligned} \tag{22}$$

where Φ_G is the ground configuration and where Φ_{Kj} is the jth configuration of the type K—local excitations, charge transfer, back charge transfer, etc. The configurational coefficients, C_G and C_{Kj}'s, are related to the elements of $\mathbf{T}^\gamma$. Variations in $\mathbf{T}^\gamma$ and hence C_{Kj}'s with the progress of reaction should delineate the mechanistic details of the reaction in question.

In what follows, we will deal with two reactions

$$CH_4 + H \rightarrow CH_3 + H_2$$

and

$$CH_2{=}CH_2 + CH_3 \rightarrow CH_2CH_2CH_3$$

along the lines described above. Significance of the results obtained will be reinforced by schematic representation of the movement of the LMO charge centroids.

II. Calculation Method

The canonical molecular orbitals (CMO) for isolated molecules as well as the entire reacting systems were calculated by the UHF method[13] in the INDO approximation.[14] The UHF LMO's were generated by the energy-localization method of Edmiston and Ruedenberg.[5] In practice, the orbital transformation matrices which minimize the exchange component of the total energy were obtained by applying the successive 2 × 2 rotation method[5] to α- and β-spin electrons separately. All possible two-orbital transformations were repeated until further increase in the sum of intraorbital Coulomb energies did not exceed 10^{-6} eV. The convergence was ascertained by applying several random transformations to the starting CMO's. Vacant CMO's were also localized by the same method.

The LMO mapping matrix $\mathbf{T}^\gamma$ was obtained by the procedure described in the preceding section. Calculations of the configurational coefficients C_{Kj} were performed by the technique[15] similar to the one used by Baba et al.[16] All computations were carried out on a FACOM 230-60 at the Kyoto University Computation Center.

III. Results of Calculation

A. Abstraction Reaction. We considered the reaction of the hydrogen atom with methane as an example of an abstraction reaction. The reaction path considered is that of the axial attack as shown in Figure 1. It involves the approach of the incoming hydrogen atom (denoted by H′) along a C–H axis of methane with subsequent departure in the opposite direction along the same axis, maintaining the C_{3v} symmetry throughout.

We specify the reaction coordinates with a notation (r_1, r_2), where r_1 is the distance in units of angstroms between the carbon atom and the hydrogen atom to be abstracted, while r_2 is the distance between this hydrogen atom and the incoming H′ atom. Calculations were carried out at six path points: A(1.1, 1.6), B(1.2, 1.1), C(1.3, 0.95), D(1.38, 0.85), E(1.5, 0.8), and F(1.7, 0.75), which are very nearly on the potential valley deduced by ab initio calculations.[17]

In the first place, we have examined how each LMO would be deformed with the progress of the reaction. It was confirmed that only the LMO's which reside over the reaction center deserve attention, the remaining LMO's being transferred from reactant to product with virtually no experience of deformation. Figure 2 schematically shows the movements of the charge centroids for the particular LMO's of our interest. The results are in harmony with the intuitive reaction mechanism of Scheme I.

Scheme I

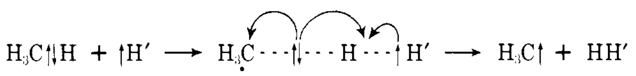

A better insight into the mechanism of bond rearrangement can be gained from the results of the LMO mapping analysis (Table I). As Table I shows, the β-spin C–H bond orbital is so deformed as to be delocalized onto the incoming H′ atom in a strongly bonding way, while the α-spin bond orbital is delocalized to a lesser extent on H′ in an antibonding way. Further, the former bond orbital allows the antibonding (C–H)* orbital to mix in with the negative sign, while the latter does so with the positive sign. The mixing of the antibonding (C–H)* into the bonding orbital (C–H) with different signs for the α- and β-spin electrons is what is called spin polarization, which is in effect equivalent to the local triplet excitation mentioned in the preceding section. In the meantime, the α-spin orbital of the incoming H′ atom first overlaps with (C–H)* and then with

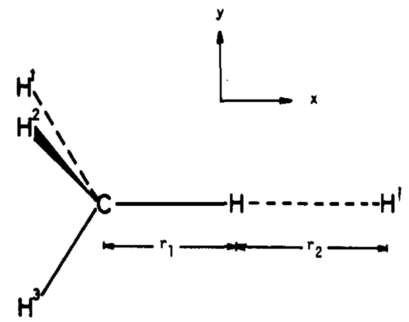

Figure 1. Coordinate system for the axial attack model of the reaction between CH_4 and H′.

Table I. LMO Mapping Analysis of the CH_4–H′ System

Spin	Path point	Mapped LMO[a]
		C–H Bond Orbital
α	(A)	0.999(CH) + 0.009(CH)* − 0.002(H′)
	(B)	0.998(CH) + 0.059(CH)* − 0.018(H′)
	(C)	0.987(CH) + 0.147(CH)* − 0.049(H′)
	(D)	0.954(CH) + 0.270(CH)* − 0.097(H′)
	(E)	0.888(CH) + 0.418(CH)* − 0.132(H′)
	(F)	0.796(CH) + 0.564(CH)* − 0.116(H′) +0.101[(CH^1) + (CH^2) + (CH^3)]
β	(A)	0.992(CH) − 0.009(CH)* + 0.126(H′)
	(B)	0.959(CH) − 0.048(CH)* + 0.278(H′)
	(C)	0.926(CH) − 0.105(CH)* + 0.362(H′)
	(D)	0.879(CH) − 0.171(CH)* + 0.442(H′)
	(E)	0.816(CH) − 0.242(CH)* + 0.522(H′)
	(F)	0.724(CH) − 0.310(CH)* + 0.614(H′)
		H′ Orbital
α	(A)	0.999(H′) − 0.039(CH)* + 0.003(CH)
	(B)	0.993(H′) − 0.110(CH)* + 0.025(CH)
	(C)	0.978(H′) − 0.192(CH)* + 0.078(CH)
	(D)	0.942(H′) − 0.282(CH)* + 0.178(CH)
	(E)	0.879(H′) − 0.362(CH)* + 0.306(CH)
	(F)	0.793(H′) − 0.429(CH)* + 0.429(CH)

[a] The bond orbitals, (CH) and (CH)*, of the isolated methane are as follows: (CH) = $0.367\chi(\mathrm{Cs}) + 0.600\chi(\mathrm{Cp}_x) + 0.710\chi(\mathrm{H}) - 0.010[\chi(\mathrm{H}^1) + \chi(\mathrm{H}^2) + \chi(\mathrm{H}^3)]$; (CH)* = $0.339\chi(\mathrm{Cs}) + 0.624\chi(\mathrm{Cp}_x) - 0.704\chi(\mathrm{H}) - 0.010[\chi(\mathrm{H}^1) + \chi(\mathrm{H}^2) + \chi(\mathrm{H}^3)]$.

(C–H). The odd electron is thus delocalized onto H in a bonding way and onto C in an antibonding manner.

The deformation of the bond orbitals should naturally be accompanied by the variation in spin density distribution. Calculated spin densities on atoms C, H, and H′ are given in Table II. Accurate values for the spin densities generally lie between the UHF results before and after spin projection.[18-20] In Table II, therefore, both the data before and after spin annihilation are listed.

The UHF ground-state wave function Ψ_{UHF} was then expanded into various component configurations at the various path points. The results are summarized in Table III. The expansion coefficients listed are for the respective lowest energy configurations of given types, which are similar to the ones used for a simple three-electron model (eq 5–13).

Inspection of Table III shows that the radical reaction proceeds by a three-stage mechanism as follows. The main driving force at the initial stage of reaction is the β-spin electron transfer (Φ_{CT}) from methane to the incoming H′ atom. At the middle stage, the back transfer (Φ_{BCT}) of the α-spin odd electron of the H′ atom to the antibonding (C–H)* orbital becomes appreciable. These two *spin delocalization stages* together contribute to the charge accumulation in the area between H and H′, to assist the formation of the H–H′ bond at sacrifice of the strength of the old C–H bond. As the reaction approaches the final stage, the contribution of the local triplet excitation ($\Phi_{LE}{}^{T}$) in the C–H bond is accelerated and becomes even the most dominant. This *spin polarization stage* is considered to be responsible exclusively for the bond cleavage. These features are believed to be common to reactions of open-shell molecules in general. The contribution of the locally excited states was ignored in a recent study by Fujimoto et al.,[21] but we would like to lay emphasis on the importance of this effect, especially in the neighborhood of the transition state.

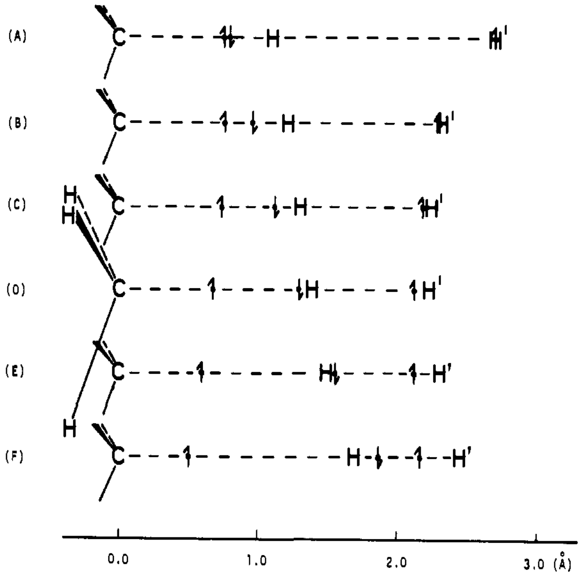

Figure 2. Schematic description of the centroids of LMO charge distributions in the abstraction reaction, $CH_4 + H' \rightarrow CH_3 + HH'$.

Table II. Variations in the Spin Densities on Atoms C, H, and H′ in the CH_4–H′ System

Path point	Spin density[a]		
	ρ_C	ρ_H	$\rho_{H'}$
(A)	0.028 (0.019)	−0.009 (−0.001)	0.982 (0.982)
(B)	0.160 (0.108)	−0.061 (−0.011)	0.909 (0.904)
(C)	0.333 (0.236)	−0.143 (−0.039)	0.827 (0.804)
(D)	0.543 (0.424)	−0.214 (−0.065)	0.700 (0.641)
(E)	0.753 (0.650)	−0.231 (−0.072)	0.517 (0.420)
(F)	0.927 (0.856)	−0.146 (−0.046)	0.266 (0.183)

[a] The values in parentheses are those after spin-annihilation.

B. Addition Reaction. The reaction studied here is the addition of the methyl radical to the double bond of ethylene, the product being the propyl radical. Since the potential surface for the reaction was thoroughly calculated by Hoyland,[22] we employed it for our purpose.

The whole aspect of the reaction can be pictorially demonstrated by schematic description of the centroids of LMO charge distributions. Figure 3 illustrates the centroids at path points (A)–(D). As the reaction proceeds, the electron pair in the banana bond (B_+) of ethylene on the side of the methyl radical becomes highly decoupled. Consequently, the β-spin electron in the bond migrates toward the methyl radical to form a new pair with the unpaired α-spin electron of the methyl radical, while the α-spin electron in the bond migrates in the opposite direction. At the same time, hybridization of the un-

Table III. Variations in the Configurational Coefficients for the Abstraction Reaction, $CH_4 + H' \rightarrow CH_3 + HH'$

Coefficient	Reaction path point (A)	(B)	(C)	(D)	(E)	(F)
C_G	0.991	0.951	0.897	0.806	0.673	0.497
C_{CT}	0.126	0.275	0.349	0.403	0.426	0.418
C_{BCT}	−0.039	−0.107	−0.186	−0.280	−0.371	−0.430
C_{LE^S}	0.000	0.007	0.018	0.034	0.050	0.061
C_{LE^T}	−0.011	−0.068	−0.151	−0.260	−0.382	−0.503
C_{LE^Q}	−0.008	−0.043	−0.089	−0.126	−0.133	−0.085
$C_{CT\text{-}LE}$	0.000	0.017	0.049	0.101	0.170	0.249
$C_{BCT\text{-}LE}$	0.000	0.000	0.021	0.054	0.109	0.183
C_{LDE}	0.000	0.000	0.014	0.039	0.079	0.126

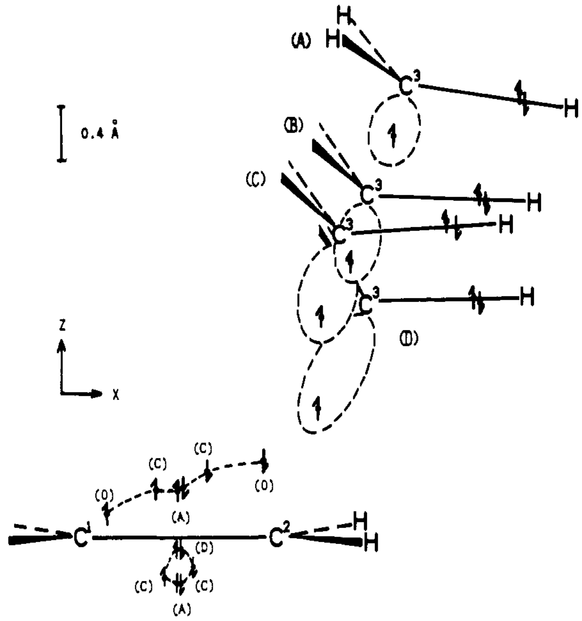

Figure 3. Schematic description of the centroids of LMO charge distributions in the addition of the methyl radical to ethylene.

paired orbital (N) of the methyl radical changes from $sp^{4.1}$ to $sp^{1.9}$. In the meantime, the paired electrons in the banana bond (B_-) on the side not facing the methyl radical are somewhat decoupled and move toward the midpoint of the double bond, thus deforming the bond from the bent type ($sp^{3.4}$) to the linear σ type ($sp^{1.4}$). These results closely agree with the conventional representation shown in Scheme II.

Scheme II

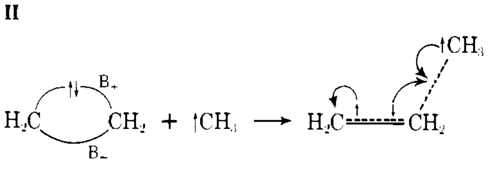

Table IV shows the results of LMO mapping analysis. As can be seen in Table IV, the α-spin B_+ orbital of ethylene is subject solely to the intramolecular deformation, while the unpaired N orbital of the methyl radical is subject to the intermolecular bond formation. The β-spin B_+ orbital suffers both types of deformation. Note that the α- and β-spin B_+ orbitals mix with B_+^* in different signs.

Table IV. LMO Mapping Analysis of the C_2H_4-CH_3 System[a]

Spin	Path point[a]	Mapped LMO
		B_+ Bond Orbital
α	(A)	$0.999B_+ - 0.000B_- + 0.002B_+^* - 0.002B_-^*$
	(B)	$0.998B_+ - 0.003B_- + 0.042B_+^* - 0.039B_-^*$
	(C)	$0.983B_+ - 0.072B_- + 0.116B_+^* - 0.108B_-^*$
	(D)	$0.711B_+ - 0.511B_- + 0.329B_+^* - 0.314B_-^*$
β	(A)	$0.999B_+ - 0.001B_- - 0.002B_+^* + 0.002B_-^* + 0.037N^*$
	(B)	$0.984B_+ - 0.012B_- - 0.037B_+^* + 0.031B_-^* + 0.169N^*$
	(C)	$0.918B_+ - 0.190B_- - 0.092B_+^* + 0.078B_-^* + 0.322N^*$
	(D)	$0.658B_+ - 0.452B_- - 0.154B_+^* + 0.148B_-^* + 0.525N^*$
		N Orbital
α	(A)	$0.999N + 0.000B_+ - 0.000B_- - 0.020B_+^* + 0.022B_-^*$
	(B)	$0.989N + 0.012B_+ - 0.011B_- - 0.101B_+^* + 0.102B_-^*$
	(C)	$0.958N + 0.057B_+ - 0.046B_- - 0.193B_+^* + 0.186B_-^*$
	(D)	$0.821N + 0.254B_+ - 0.195B_- - 0.311B_+^* + 0.305B_-^*$

[a] For the coordinate system, see Figure 3. [b] $B_\pm$ and $B_\pm^*$, respectively, denote the bonding and antibonding banana bonds of isolated ethylene: $B_\pm = 0.339[\chi(C^1s) + \chi(C^2s)] + 0.368[\chi(C^1p_x) - \chi(C^2p_x)] \pm 0.500[\chi(C^1p_z) + \chi(C^2p_z)] - 0.002[\chi(H^1) + \chi(H^2) + \chi(H^3) + \chi(H^4)]$; $B_\pm^* = 0.322[\chi(C^1s) - \chi(C^2s)] + 0.383[\chi(C^1p_x) + \chi(C^2p_x)] \pm 0.500[\chi(C^1p_z) - \chi(C^2p_z)] - 0.010[\chi(H^1) + \chi(H^2) - \chi(H^3) - \chi(H^4)]$. N and N* stand for the occupied and vacant unpaired orbitals of the methyl radical, respectively, which have the following forms at path point (A), for example: $N = 0.435\chi(C^3s) - 0.256\chi(C^3p_x) - 0.858\chi(C^3p_z)$; $N^* = 0.165\chi(C^3s) - 0.282\chi(C^3p_x) - 0.942\chi(C^3p_z)$.

Inspection of Table IV shows that the mapping coefficients for the antibonding orbitals B_+^* and B_-^* are mutually in different signs and nearly identical in magnitude at every path point. This indicates that the customary antibonding π orbital

$$\pi^* = [\chi(C^1p_z) - \chi(C^2p_z)]/\sqrt{2} = [B_+^* - B_-^*]/\sqrt{2} \quad (23)$$

is responsible for the deformation of the three LMO's under consideration. Bearing this in mind, one may notice in Table IV the following succession of bond deformation: (1) The β-spin B_+ bond first starts to delocalize onto the methyl group; (2) the methyl N orbital is so deformed as to be delocalized over the π^* orbital of ethylene; and (3) local triplet excitation, i.e., spin polarization, of the ethylene π bond becomes appreciable.

Listed in Table V are the total weights of various types of

Table V. Total Weights of the Composite Configurations in the Addition of Methyl Radical (M) to Ethylene(E)

Path point[a]	Spin	C_G^2 (EM)	$\sum_i C_{LE,i}^2$ (E*M)	$\sum_k C_{CT,k}^2$ (E^+M^-)	$\sum_l C_{BCT,l}^2$ (E^-M^+)	$\sum_j C_{LE,j}^2$ (EM*)
(A)	α		0.000	0.000	0.001	0.000
	β		0.000	0.003	0.000	0.000
	Sum	0.996	0.000	0.003	0.001	0.000
(B)	α		0.006	0.001	0.021	0.000
	β		0.004	0.056	0.001	0.001
	Sum	0.909	0.010	0.057	0.022	0.001
(C)	α		0.036	0.003	0.076	0.001
	β		0.017	0.125	0.001	0.004
	Sum	0.729	0.053	0.128	0.077	0.005
(D)[b]	α		0.103	0.006	0.209	0.001
	β		0.024	0.187	0.001	0.010
	Sum	0.407	0.127	0.193	0.210	0.011

[a] The path points (A)-(D) are indicated in Figure 3. [b] Other highly transferred and highly excited configurations are also mixed into the configuration Φ_G(EM) to some extent. The weights of these configurations are not given here, however.

configurations K contributing to Ψ_{UHF} at different reaction path points. It can be seen here also that the reaction proceeds by way of the successive β- and α-spin electron transfers followed by the local triplet excitation of ethylene. The first two spin delocalization stages are responsible for the formation of a new bond between one of the ethylene carbons and the methyl radical and for weakening the old banana bond B_+. The last spin polarization stage is considered to be responsible for the cleavage of the banana bond. The interchange of the pairings of opposite spins takes place smoothly via these stages.

IV. Discussion

The main conclusion of this work is that both the abstraction and addition reactions of radicals are considered to proceed through a three-stage mechanism. The course of reaction should depend on how smoothly the interchange of the pairings of opposite spins could take place.

A brief comment on the relationship between the interchange of spin pairings in our three-stage mechanism and the implication of the conventional orbital correlation diagrams may be worthwhile. The most dominant orbital interactions at an intermediary stage of radical reaction are as illustrated in Figure 4. Obviously, the interaction of a doubly occupied orbital of substrate with a singly occupied orbital of radical results in the stabilization of the former orbital and the destabilization of the latter. As a result, the energy level for the singly occupied orbital approaches that of a vacant orbital of the substrate. With further progress of reaction a crossing of these two energy levels may take place (Figure 4a). When the interaction of the singly occupied orbital with the vacant orbital (and hence the back charge transfer from radical to substrate) is permissible for some geometrical reason, the two orbitals are stabilized and destabilized, respectively, and hence the crossing of the two energy levels can be avoided (Figure 4b). Thus, the occurrence of a smooth interchange of spin pairings in the three-stage process is in a sense equivalent to an avoidance of the orbital crossing in the orbital correlation diagram.[23] No doubt, an intermediary stage involving both the forward and back charge transfer processes is more stabilized energetically as compared with that involving only the forward charge transfer process.[24] In addition, the nodal character of the singly occupied orbital should be conserved in Figure 4b, while it is generally not in Figure 4a.

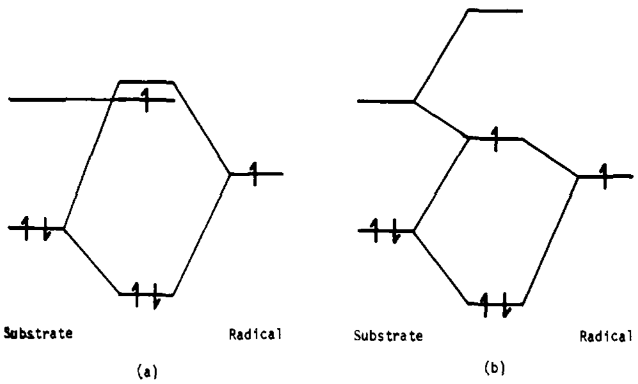

Figure 4. Orbital interaction diagrams for radical reactions. (a) Only the charge transfer from substrate to radical is permissible. (b) Both the charge transfer and back charge transfer are permissible.

The back charge transfer (BCT) process should thus play an important role in determining the course of addition and abstraction reactions.[25] In the case of the reaction between CH_4 and H′, the BCT apparently favors the axial approach (Figure 1) of reactants. If the incoming H′ atom approached methane by way of the insertion-like motion with a large angle to the C–H axis of methane, the contribution of the back α-spin electron transfer would be reduced considerably because of the diminishing intermolecular overlap of the LMO's associated with the interaction. The new bond formation, i.e., the new pairing of opposite spins, would then be seriously obstructed. These expectations were confirmed by separate calculations.[25]

Similar considerations apply to the reaction of methyl radical with ethylene. The methyl radical initially approaches ethylene along the perpendicular bisector of the double bond because of the dominant contribution of the β-spin electron delocalization from ethylene to the methyl radical. With the progress of reaction, however, it should veer to one side of the space in search of a path favorable for the back α-spin delocalization and the concomitant spin polarization. Consequently, the central attack to the double bond is considered to be less favorable.

Generally speaking, if no pathway favorable for the BCT can be found during reaction, the reaction will not proceed easily despite the existing charge transfer. Back charge transfer seems to be an important factor in determining the course of reactions.[26]

Conclusions

The UHF-LMO description of chemically interacting systems provides useful pictures of deformation and rearrangement of bonds involved in chemical reactions of species with unpaired electron spins. The LMO mapping analysis shows that only the LMO's which constitute the reaction centers suffer appreciable deformation during reaction; other LMO's have great transferability. Chemical reactions can thus be deemed as local properties of reactant molecules. The particular LMO's associated with reaction centers reveal a pattern that the reactions of open-shell molecules proceed through a three-stage mechanism. The successive β- and α-spin electron transfers which take place between reactant molecules should lead to a new electron-pair bond via a three-center bond. The concomitant spin polarization of the old bond plays an important role in the cleavage of that bond. The whole aspect of the reactions is well in accord with the customarily accepted mechanistic scheme. In conclusion, the UHF-LMO treatments do not only shed light on the mechanism of radical reactions, but provide a sound theoretical foundation for conventional concepts already familiar in chemistry.

References and Notes

(1) M. J. Feinberg and K. Ruedenberg, *J. Chem. Phys.*, **54**, 1495 (1971).
(2) R. F. W. Bader and H. J. T. Preston, *Int. J. Quant. Chem.*, **3**, 327 (1969).
(3) C. W. Wilson and W. A. Goddard III, *Theor. Chim. Acta*, **26**, 195, 211 (1972).
(4) J. E. Lennard-Jones and J. A. Pople, *Proc. R. Soc. London, Ser. A*, **210**, 190 (1951).
(5) C. Edmiston and K. Ruedenberg, *Rev. Mod. Phys.*, **35**, 457 (1963); *J. Chem. Phys.*, **43**, 597 (1965).
(6) K. F. Purcell and T. G. M. Doph, *J. Am. Chem. Soc.*, **94**, 2693 (1972).
(7) A. Dedieu and A. Veillard, *J. Am. Chem. Soc.*, **94**, 6730 (1972).
(8) D. A. Dixon and W. N. Lipscomb, *J. Am. Chem. Soc.*, **95**, 2853 (1973).
(9) D. M. Hirst and M. E. Linington, *Theor. Chim. Acta*, **16**, 55 (1970).
(10) S. L. Guberman and W. A. Goddard III, *J. Chem. Phys.*, **53**, 1803 (1970).
(11) K. F. Purcell and W. C. Danen, *J. Am. Chem. Soc.*, **94**, 7613 (1972).
(12) C. Trindle, *J. Am. Chem. Soc.*, **92**, 3251, 3255 (1970).
(13) J. A. Pople and R. K. Nesbet, *J. Chem. Phys.*, **22**, 571 (1954).
(14) J. A. Pople, D. L. Beveridge, and P. A. Dobosh, *J. Chem. Phys.*, **47**, 2026 (1967).
(15) The expansion coefficients obtained by the present UHF method will be somewhat different from those obtained by the variational configuration interaction method or by the spin-extended Hartree-Fock method, which minimizes the total energy after spin-projection. However, the differences are not so large as to affect seriously the conclusion of this work.
(16) H. Baba, S. Suzuki, and T. Takemura, *J. Chem. Phys.*, **50**, 7078 (1969).
(17) K. Morokuma and R. E. Davis, *J. Am. Chem. Soc.*, **94**, 1060 (1972).
(18) L. C. Snyder and A. T. Amos, *J. Chem. Phys.*, **42**, 3670 (1965).
(19) A. T. Amos and M. Woodward, *J. Chem. Phys.*, **50**, 119 (1969).
(20) A. T. Amos and B. L. Burrows, *J. Chem. Phys.*, **52**, 3072 (1970).
(21) H. Fujimoto, S. Yamabe, T. Minato, and K. Fukui, *J. Am. Chem. Soc.*, **94**, 9205 (1972).
(22) J. R. Hoyland, *Theor. Chim. Acta*, **22**, 229 (1971).
(23) In the state correlation diagram, the smooth interchange of spin pairings is considered to be related with the noncrossing of diabatic bases Φ_G and Φ_{LE}^T.
(24) As can be conjectured from Figure 4, the back charge transfer process will be much more important in the case of nucleophilic reactions, but immaterial in the case of electrophilic reactions.
(25) In the case of the insertion-like approach, the contribution of the spin polarization was also greatly reduced, and identical α-spin densities were induced at the two ends of the substrate bond.
(26) Importance of the steric effects (exchange-repulsion interactions) has been considered by T. Fueno, S. Nagase, K. Tatsumi, and K. Yamaguchi, *Theor. Chim. Acta*, **26**, 43 (1972); S. Nagase and T. Fueno, *ibid.*, **35**, 217 (1974).

Solid State Polymerization of S_2N_2 to $(SN)_x$[1]

Marshall J. Cohen,[2a,c] A. F. Garito,[2a,c] A. J. Heeger,[2a,c] A. G. MacDiarmid,*[2b,c] C. M. Mikulski,[2b,c] M. S. Saran,[2b,c] and J. Kleppinger[2b,c]

Contribution from the Departments of Physics and Chemistry and Laboratory for Research on the Structure of Matter, University of Pennsylvania, Philadelphia, Pennsylvania 19174.

Received September 18, 1975

Abstract: A model of the solid state polymerization of S_2N_2 to $(SN)_x$ is presented using x-ray structure results for S_2N_2, $(SN)_x$, and a crystal of S_2N_2 which has been allowed to partially polymerize. $(SN)_x$ has the monoclinic space group $P2_1/c$ with two crystallographically equivalent chains per unit cell and two SN units per chain: $a = 4.153$ (6), $b = 4.439$ (5), $c = 7.637$ (12) Å, with $\beta = 109.7$ (1)°. The structure of a single chain consists of nearly equal bond lengths with successive values of 1.593 (5) and 1.628 (7) Å; the NSN and SNS bond angles are 106.2 (2)° and 119.9 (4)°, respectively. S_2N_2 forms in the monoclinic space group $P2_1/c$ with two S_2N_2 molecules per unit cell: $a = 4.485$ (2), $b = 3.767$ (1), $c = 8.452$ (3) Å, with $\beta = 106.43$ (3)°. The S_2N_2 molecule is cyclic and nearly square planar with SN bond lengths of 1.657 (1) and 1.651 (1) Å and NSN and SNS bond angles of 89.58 (6)° and 90.42 (6)°, respectively.

I. Introduction

The past 2 years have witnessed a remarkable growth of interest in polymeric sulfur nitride, $(SN)_x$. In 1973, Labes and co-workers[3a] reported on experimental studies of the electrical transport properties which suggested that $(SN)_x$ was metallic. Heat capacity measurements[3b] in the pumped helium temperature range were consistent with metallic behavior. Since $(SN)_x$ was known to be a polymer, the electronic properties were assumed to be one dimensional. This assumption coincided with the current interest in the properties of one-dimensional systems exemplified by the charge-transfer salts of (TCNQ)[4] and the platinum-chain salts.[5]

Experimental studies on pure material verified the metallic behavior and demonstrated that it is possible to vacuum deposit oriented epitaxial films of $(SN)_x$ on a wide range of polymer substrates.[6] These films have a high optical anisotropy throughout the near infrared and the low-frequency portion of the visible spectrum suggesting possible applications in optical devices. $(SN)_x$ remains metallic to very low temperatures and becomes superconducting near 0.3 K,[7] thus extending the phenomenon of superconductivity into a new region of the periodic table.

Experimental studies[3,7-9] have shown no indication of the instabilities expected for pseudo-one-dimensional systems. Moreover, optical studies on single crystals and epitaxial films[6b] imply that $(SN)_x$ is not to be regarded as a one-dimensional, but as an anisotropic two- or possibly three-dimensional, metal. These experimental studies thus suggest relatively strong interactions between polymer chains.

In this communication we report detailed structural information on[10] $(SN)_x$ obtained using x-ray techniques together with the x-ray determined structures of S_2N_2 and of a crystal of S_2N_2 which has been allowed to partially polymerize. Using these data, a model of the solid state polymerization of S_2N_2 to $(SN)_x$ is proposed and discussed. The polymerization process implies relatively strong interactions between chains in the $(SN)_x$ crystal structure.